turnovers per minute, respectively. Under identical conditions, but with RhTTPI as the catalyst, the rates are 9.1 and 28.6 turnovers per minute, respectively, a larger difference between rates. Thus, the unusual kinetic behavior of the RhTTPI-catalyzed reactions can be attributed to the fact that the alkene acts as an axial ligand and influences the rate of metallocarbene formation (*13*). Our observation that a rhodium alkyl complex (perhaps the alkene complex of **1**) is the dominant steady-state intermediate in the catalytic reaction argues that the major effect is that of substrate acceleration of nitrogen ejection, but more work will be required to address this point rigorously. The fact that CH_3RhTTP is an efficient catalyst provides further evidence that nucleophilic attack on a metal-alkene complex (Eq. 2) is not an important reaction pathway.

Our current understanding of the catalytic cycle is summarized in Fig. 5. Our experiments strongly support the metallocarbene mechanism for metal-catalyzed cyclopropanation reactions. The direct precursor to a rhodium porphyrin carbene, the diazoalkyl complex **1**, has been characterized, and its thermal decomposition chemistry has been examined. Furthermore, kinetic and spectroscopic investigations have shown that alkene π complexes play a role in the catalytic process by influencing the rate of metallocarbene formation.

REFERENCES AND NOTES

1. A. P. Marchand and N. MacBrockway, *Chem. Rev.* **74**, 431 (1974); E. Wenkert, *Acc. Chem. Res.* **13**, 27 (1980); M. P. Doyle, in *Catalysis of Organic Reactions*, R. L. Augustine, Ed. (Dekker, New York, 1985), chap. 4; E. Wenkert, *Heterocycles* **14**, 1703 (1980); H. Fritschi, U. Leutenegger, A. Pfaltz, *Angew. Chem. Int. Ed. Engl.* **25**, 1005 (1986); R. E. Lowenthal, A. Abiko, S. Masamune, *Tetrahedron Lett.* **42**, 6005 (1990); D. A. Evans, K. A. Worpel, M. M. Hinman, *J. Am. Chem. Soc.* **113**, 726 (1991); M. P. Doyle *et al.*, *Tetrahedron Lett.* **46**, 6613 (1990); M. P. Doyle *et al.*, *J. Am. Chem. Soc.* **113**, 1423 (1991); J. L. Maxwell, S. O'Malley, K. C. Brown, T. Kodadek, *Organometallics* **11**, 645 (1992).
2. M. P. Doyle, *Chem. Rev.* **86**, 919 (1988).
3. Metal carbenes that cyclopropanate alkenes stoichiometrically are known. For a review, see M. Brookhart and W. B. Studabaker, *ibid.* **87**, 411 (1987).
4. D. S. Wulfman, R. S. McDaniel, B. W. Peace, *Tetrahedron* **32**, 1241 (1976); R. G. Salomon and J. K. Kochi, *J. Am. Chem. Soc.* **95**, 3300 (1973); A. J. Anciaux, J. A. Hubert, A. F. Noels, N. Petiniot, P. Teyssie, *Tetrahedron Lett.* **1973**, 2233 (1973); A. Nakamura, T. Koyama, S. Otsuka, *Bull. Chem. Soc. Jpn.* **51**, 593 (1978); A. Nakamura, A. Konishi, R. Tsujitani, M. Kudo, S. J. Otsuka, *J. Am. Chem. Soc.* **100**, 3449 (1978).
5. J. P. Collman, L. S. Hegedus, J. R. Norton, R. G. Finke, *Principles and Applications of Organotransition Metal Chemistry* (University Science, Mill Valley, CA, 1987), pp. 825–858.
6. H. J. Callot, F. Metz, C. Piechocki, *Tetrahedron* **38**, 2365 (1982).
7. When equimolar amounts of EDA and RhTTPI were mixed at 25°C in an evacuated flask and the solution was then cooled to −40°C, analysis of the headspace by gas chromatography revealed the presence of 1 equivalent of nitrogen gas.
8. The band corresponding to the diazo stretch in EDA is located at 2335 cm^{-1} (CH_2Cl_2 solution sandwiched between CaF_2 plates). This is different from the value observed with NaCl plates (2115 cm^{-1}). The position of the diazo stretch in the EDA-porphyrin complex is in the range expected for a transition metal–alkyldiazonium complex [see H. Konig, M. J. Menu, M. Dartiguenave, Y. Dartiguenave, H. F. Klein, *J. Am. Chem. Soc.* **112**, 5351 (1990), and references therein for a description of related metal-diazoalkyl species].
9. H. J. Callot and J. Schaeffer, *J. Chem. Soc. Chem. Commun.* **1978**, 937 (1978).
10. J. L. Maxwell and T. Kodadek, *Organometallics* **10**, 4 (1991).
11. Like most metal-catalyzed cyclopropanation reactions, the rhodium porphyrin–catalyzed reaction produces some carbene dimers (cis and trans isomers of $EtO_2CCH{=}CHCO_2Et$; Et, ethyl). We presume that these products result from nucleophilic attack by EDA on the metallocarbene, a reaction that competes with carbene transfer to the alkene. As the EDA concentration is increased or the alkene concentration is reduced, the ratio of dimer product to cyclopropane grows. Because formation of the carbene dimer consumes 2 equivalents of EDA, the rate of the cyclopropanation reaction will deviate somewhat from ideal first-order behavior. The differences in the apparent rates of cyclopropanation of styrene and 1-decene are not due simply to differences in selectivity (moles of cyclopropane per moles of EDA consumed). The rates presented in the text have been corrected for differences in the selectivity.
12. Porphyrin metal-alkene and metal-alkyne π complexes have been characterized for other metals. L. K. Woo, J. A. Hays, R. A. Jacobson, C. L. Day, *Organometallics* **10**, 2102 (1991); J. P. Collman, P. J. Brothers, L. McElwee-White, E. Rose, *J. Am. Chem. Soc.* **107**, 6110 (1985); J. P. Collman, C. E. Barnes, L. K. Woo, *Proc. Natl. Acad. Sci. U.S.A.* **80**, 7684 (1983).
13. Because the ester and diazo substituents of **1** are highly electron withdrawing, the $CH(N_2)^+(CO_2Et)$ ligand is expected to have a much more modest trans effect than the methyl group. Therefore, we expect that **1** can also form alkene complexes.

14. Supported by American Chemical Society–Petroleum Research Fund grant 24052-AC1. T.K. also acknowledges the American Cancer Society for a Junior Faculty Research Award. We thank T. Mallouk for the use of his gas chromatograph and infrared spectrometer and M. Darensbourg for the loan of a low-temperature infrared cell.

18 February 1992; accepted 21 April 1992

Glassy Microspherules (Microtektites) from an Upper Devonian Limestone

Kun Wang

The properties of microspherules recovered from an Upper Devonian marine limestone immediately overlain by a geochemical anomaly of siderophile and chalcophile elements are similar to those of impact-derived microtektites. These microspherules are glass, have splash-form shapes, contain spherical vesicles and lechatelierite inclusions, and show oxide compositional variations similar to those in known microtektites. These characteristics suggest that these Upper Devonian microspherules have an impact origin. A bolide impact may have occurred about 365 million years ago on the South China Plate and caused a faunal extinction on eastern Gondwana.

Recognition of ancient bolide impacts and their influence on biota is important for understanding the evolution of Earth and its biosystem. Signatures of an impact in the pre-Cenozoic rock record are difficult to recognize because of their long history. Microspherules were discovered in a marine limestone from the Upper Devonian conodont lower *Palmatolepis crepida* zone in South China (*1*). Chemostratigraphic and paleontological studies indicate that a geochemical anomaly, a negative carbon isotope excursion, and a brachiopod faunal turnover are associated with the occurrence of the microspherules in South China (Figs. 1 and 2) (*2*). Geochemical anomalies (iridium and carbon isotope) were found in the same conodont zone in Western Australia (*3*). On the basis of these results and the presence of a probable Late Devonian impact crater under Taihu Lake in South China (Fig. 1) (*4*), we propose that a bolide impact occurred about 365 million years ago on the South China Plate and probably caused a regional extinction in the Southern Hemisphere (eastern Gondwana) (*2*). In this paper, I describe glassy microspherules from South China and provide evidence that they are of impact origin.

Microspherules were recovered from a marine limestone that is immediately below a geochemical anomaly that occurs in a 3-cm-thick claystone between the Shetianqiao and Xikuangshan formations at Qidong, Hengyang, Hunan Province, South China (Figs. 1 and 2). The Qidong section, exposed in a quarry behind an elementary school about 1.5 km east of the center of the small town, was sampled when the quarry was being mined by local residents for paving stones. Samples from 25 stratigraphic horizons were collected over a 20-m span along a fresh exposure of the section. The samples were cleaned and then dissolved in 10% acetic acid. Conodonts and microspherules were picked from the 60- to 250-μm size fraction of the sieved residues. Microspherules were found only in the residues from one

Department of Geology, University of Alberta, Edmonton, Alberta, Canada T6G 2E3.

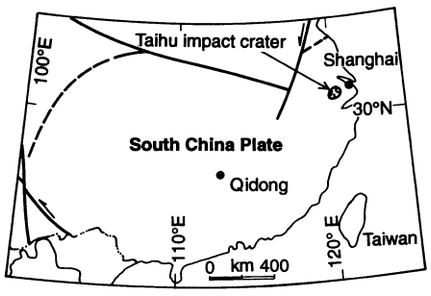

Fig. 1. Tectonic map of the South China Plate with locations of the Qidong microspherules and the Taihu Lake impact crater. The two localities are about 900 km apart.

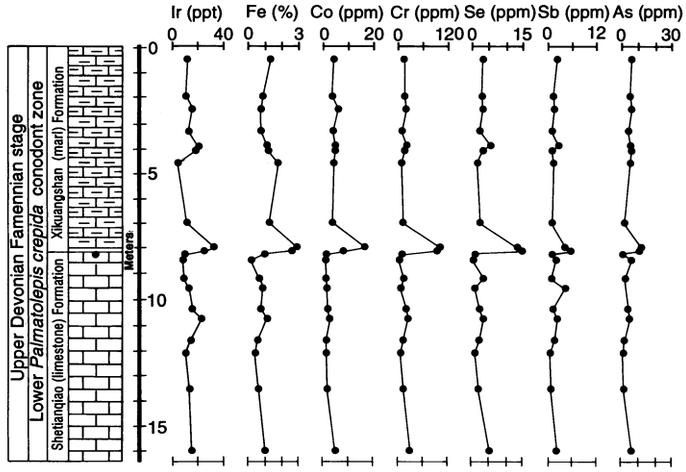

Fig. 2. Chemostratigraphy of the Qidong section showing a geochemical anomaly of siderophile and chalcophile elements in a 3-cm-thick claystone (50% illite, 25% calcite, 25% quartz) between the two formations. The claystone is immediately above the limestone that contains the microspherules (indicated by a solid circle in the stratigraphic column).

horizon (5), which is immediately below the geochemical anomaly that was revealed later by neutron activation analysis (Fig. 2). Conodonts from the section indicate that the microspherules occur in the lower *P. crepida* zone (6), which is three zones above (or about 1.5 million years after) the Frasnian-Famennian boundary extinction event in South China (7).

About 60 microspherules were picked and studied in detail. The microspherules range from 80 to 160 μm in diameter; most are ~100 μm across. Although most are spherical, a few are in the form of a teardrop or a pear, with a protruding tail (Fig. 3). These so-called "splash-form" shapes are the most common form in known microtektites (8). Some specimens have two or more spherules welded together by material that has a chemical composition similar to that of the spherules and is probably derived from the same parental material (Fig. 3D). The microspherules vary in translucence and color. They are opaque white, translucent dark brown, or transparent yellowish brown, but a few are colorless and transparent. Surface textures vary from smooth with a glassy luster to pitted and corroded with a dull or frosted luster. Elevated small caps were also observed (Fig. 3, B and D). Broken fragments of the microspherules showed a conchoidal fracture when two specimens were crushed. The appearance of the microspherules is similar to that of known microtektites (8).

Petrographically, the microspherules are isotropic, except for a few quartz inclusions present in some specimens. X-ray microdiffraction (XRMD) (9) performed on individual specimens confirmed that the microspherules are amorphous; the only mineral phase identified in the XRMD patterns was quartz (Fig. 4). Application of the oil-immersion technique to four fragments from two microspherules gave refractive indices ranging between 1.544 and 1.548; this is consistent with tektite glass having ~61 to 65% SiO_2 (10).

Energy-dispersive x-ray analysis was performed on all of the microspherules. All showed a silicate composition; Si, Al, Ca, Fe, K, Na, and Mg were the major elements. Analysis of seven randomly selected microspherules with an electron microprobe (11) revealed that the microspherules contain up to three phases: a matrix glass ($SiO_2 \approx 62\%$), a high-silica glass ($SiO_2 \approx 86\%$), and pure silica inclusions ($SiO_2 > 99\%$) (Table 1). The matrix glass is dominant and some microspherules are made up entirely of this material (Fig. 5A). The other two phases, when present, occur as isolated SiO_2-rich areas in the matrix glass (Fig. 5B). These areas appeared darker than matrix glass under the microprobe. Petrographically, the pure silica inclusions are largely isotropic and partially crystalline. The isotropic pure silica inclusions have a lower refractive index than the surrounding glass; they are lechatelierite (SiO_2 glass). The crystalline silica inclusions are quartz. Silica inclusions were found in three of the seven microspherules analyzed. Some North American microtektites and Muong Nong type tektites also contain inclusions of quartz and lechatelierite (12). It is widely held that lechatelierite particles in tektites were formed by the melting of quartz grains during an impact (13). The presence of both lechatelierite and quartz inclusions is probably a result of the partial melting of quartz grains in the molten melt that had a temperature near the melting point of quartz. The presence of spherical vesicles in

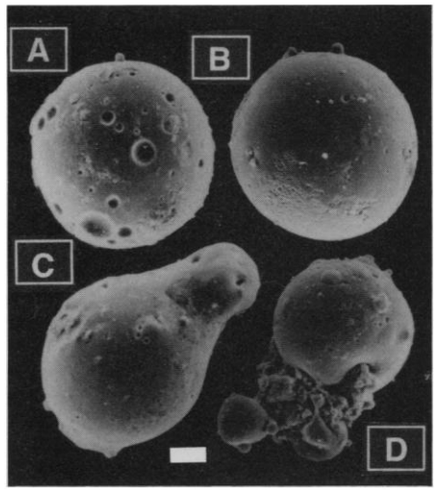

Fig. 3. Scanning electron micrographs of surfaces of the Qidong microspherules. (**A**) Surface with "crater-like" big shallow pits and caps. (**B**) Finely pitted surface with two caps on the top. (**C**) Pear-shaped spherule with a few small pits. (**D**) Welded spherule with caps on the surface that is slightly pitted (welding material = impact melt?). Caps are composed of silica as revealed by energy-dispersive x-ray analysis. Scale bar, 20 μm.

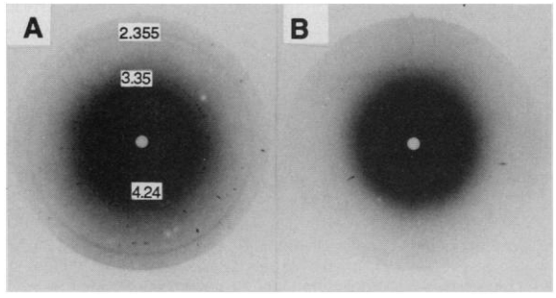

Fig. 4. X-ray microdiffraction patterns of the Qidong microspherules. (**A**) Pattern showing that the only crystalline phase in this microspherule is quartz (3.35 Å, 4.24 Å); sample-to-film distance was corrected with the d_{111} (2.355 Å) of gold used as the internal standard. (**B**) Amorphous pattern of a purely glassy microspherule. For comparison, an Australasian tektite was also analyzed and it showed the same amorphous pattern as in (B). Film exposure times for these analyses were between 24 and 48 hours.

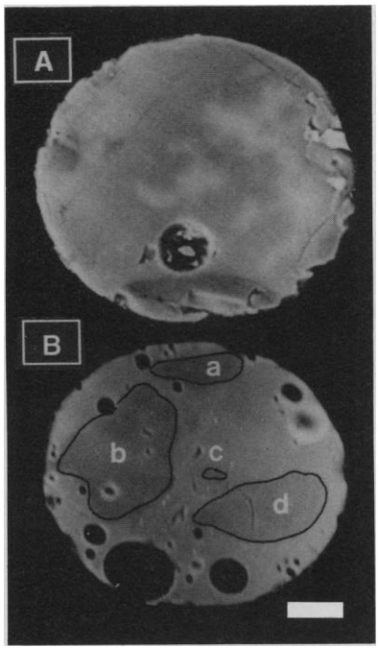

Fig. 5. Scanning electron micrographs in the backscattered mode of polished sections of the Qidong microspherules. (**A**) Rather homogeneous glassy spherule with a vesicle. (**B**) Inhomogeneous spherule showing vesicles (black holes) and silica-rich areas (a, b, c, and d) within a glass matrix: a, high-silica glass (see Table 1); b, high-silica glass (25%) + silica glass (50%) + quartz (25%); c, quartz; d, silica glass (80%) + quartz (20%) (modal estimates). Small bright spots are burns caused by the electron beam during microprobe mapping. Scale bar, 20 μm.

Fig. 6. Oxide compositional variation diagram comparing the Qidong microspherules (crosses) to microtektites from three known strewn fields: North America (triangles) (*20*), Australasia (squares) (*21*), and Ivory Coast (circles) (*22*). Note the excellent correlations between SiO_2 and Al_2O_3 (r = 0.97), and between SiO_2 and CaO (r = 0.87), for the microspherules.

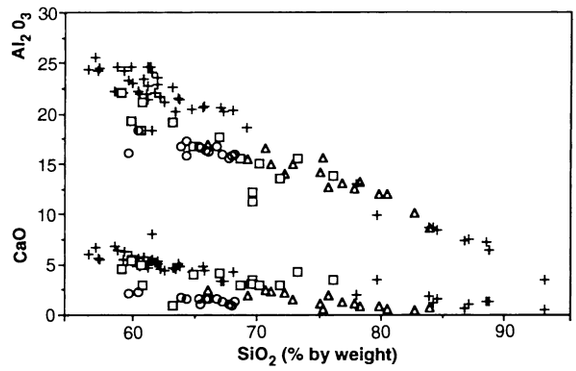

Table 1. Major oxide composition of the Qidong microspherules. Data are in percent by weight based on 80 microprobe analyses (50 on matrix glass, 10 on high-silica glass, and 20 on silica inclusions) performed on seven randomly selected specimens.

Oxide	Matrix glass		High-silica glass		Silica inclusions*	
	Average	Range (%)	Average	Range (%)	Average	Range (%)
SiO_2	61.77	58.19–67.16	86.33	79.79–93.04	99.68	99.3–100.45
Al_2O_3	21.82	20.58–24.01	7.38	3.53–9.96	0.19	0.00–0.39
FeO†	1.48	0.46–2.80	0.56	0.33–1.15	0.02	0.00–0.04
MgO	2.91	1.15–4.14	0.71	0.31–1.65	0.01	0.00–0.03
CaO	5.15	3.37–6.83	1.45	0.56–3.54	0.02	0.00–0.04
K_2O	3.23	2.66–4.45	1.97	1.29–2.71	0.05	0.00–0.11
Na_2O	2.48	2.31–2.70	1.08	0.59–1.41	0.00	0.00–0.01
TiO_2	0.55	0.20–0.70	0.24	0.14–0.55	0.07	0.00–0.33
MnO	0.04	0.00–0.09	0.02	0.00–0.07	0.01	0.00–0.05
Cr_2O_3	0.05	0.00–0.14	0.05	0.00–0.15	0.00	0.00–0.00
Total	99.48		99.79		100.05	

*Silica inclusions are largely isotropic (lechatelierite) and partially crystalline (quartz). †All Fe expressed as FeO.

the microspherules implies their original molten state.

The chemical compositions of the microspherules are given in Table 1. A plot of SiO_2 versus other major oxides for the microspherules indicates that Al_2O_3, CaO (Fig. 6), MgO, TiO_2, and FeO all decrease with increasing SiO_2. The microspherules show oxide variation trends similar to those in known microtektites (Fig. 6) (*14*). North American microtektites plotted in Fig. 6 appear to fill the gap between the matrix glass and the high-silica glass on the trends for the Qidong microspherules; FeO is the only oxide in the microspherules that falls off the variation trend of North American microtektites. This may reflect a slightly different, iron-poorer source material for the microspherules.

Like known microtektites, the microspherules are volatile-poor as is evident from their high oxide totals. The microspherule glasses survived 365 million years undevitrified, suggesting that they must have contained very little water (*15*). In contrast, volcanic glass shards found in marine sediments tend to be water-rich (*16*). Except for quartz, the microspherules are devoid of microlites and other minute crystals commonly found in volcanic glasses. The microspherules contain lechatelierite, but volcanic glasses do not (*13*). These observations essentially exclude the possibility that the microspherules are of volcanic origin.

Survival of the microspherules for 365 million years implies that there is an unusual preservation mechanism that prevented devitrification of the glass (*15*, *17*). Preservation of the microspherules may have been aided by their inclusion in a diagenetic limestone (*18*). Early diagenesis may have greatly reduced the permeability of the limestone and thus shielded the microspherules from fluid interaction, thus preventing devitrification. The Qidong section may never have been deeply buried.

The microspherules closely resemble microtektites in many respects. On the basis of their physical and chemical characteristics, such as the splash-form shapes, the presence of spherical inner vesicles, the presence of lechatelierite, the absence of primary crystallites (except for a few quartz inclusions in some specimens), and variations in chemical composition similar to those in microtektites (*19*), I suggest that the Qidong microspherules are Upper Devonian microtektites. A probable Late Devonian impact crater under Taihu Lake on the South China Plate could have been the impact site (Fig. 1) (*4*).

REFERENCES AND NOTES

1. K. Wang, *Geol. Soc. Am. Abstr. Programs* **23**, A277 (1991). The conodont lower *P. crepida* zone has an age of about 365 million years; each Upper Devonian conodont zone represents a duration of less than 0.5 million years [W. Ziegler and C. A. Sandberg, *Courier Forschungsinstitut Senckenberg* **121**, 7 (1990)].
2. K. Wang and H. H. J. Geldsetzer, paper presented at the 5th International Conference on Global Bio-Events: Phanerozoic Bio-Events and Event Stratigraphy, Göttingen, Germany, 16 to 19 February 1992; in preparation.
3. An iridium anomaly (about 20 times the background value) was originally reported in the conodont upper *P. triangularis* zone in the Canning Basin, Western Australia [P. E. Playford, D. J. McLaren, C. J. Orth, J. S. Gilmore, W. D. Goodfellow, *Science* **226**, 437 (1984)]. An evaluation of the conodont fauna showed that the iridium anomaly is actually in the subsequent lower *P. crepida* zone [R. S. Nicoll and P. E. Playford, *Geol. Soc. Aust. Abstr. Ser.* **21**, 296 (1988)].
4. Abundant shocked quartz grains have been found from the Wutong Formation quartzite of the Upper Devonian in the Taihu Lake area [Y-N. He *et al.*, *Chinese Sci. Bull.* **36**, 848 (1991)]. Recent work indicates that the impact crater is probably substantially larger than the diameter of the lake (70 km), as shock effects are observed 30 km outside the lake (V. L. Sharpton, D. Y. Xu, D. F. Lu, in preparation).
5. All samples were processed in the same fashion

at the same time in the same laboratory, but no microspherules were observed in the samples from the other 24 horizons. There are no signs of contamination of the samples at the outcrop or in the laboratory.
6. K. Wang and S. Bai, *Can. Soc. Petrol. Geol. Mem.* **14** (no. 3), 71 (1988); Q. Ji, *Courier Forschungsinstitut Senckenberg* **117**, 276 (1990).
7. K. Wang *et al.*, *Geology* **19**, 776 (1991).
8. B. P. Glass, *Geol. Soc. Am. Bull.* **85**, 1305 (1974).
9. F. J. Wicks and J. Zussman, *Can. Mineral.* **13**, 244 (1975).
10. The refractive index of natural glasses varies inversely with SiO_2 content [L. G. Berry, B. Mason, R. V. Dietrich, *Mineralogy* (Freeman, New York, ed. 2, 1983), p. 542]. A plot of the refractive indices of tektites versus their SiO_2 concentrations showed that they define a curve that lies above the curve for igneous glasses [B. P. Glass, *Geochim. Cosmochim. Acta* **33**, 1135 (1969); G. A. Izatt, *J. Geophys. Res.* **96**, 20879 (1991)]. The refractive index of the Qidong microspherules plotted against the analyzed SiO_2 concentration also lies above the curve for igneous glasses.
11. Included are both random point analyses and more detailed elemental mapping. Instrument conditions are as follows: accelerating potential, 15 kV; probe current on brass, 8.5 nA; count time, 20 s; and ZAF correction.
12. B. P. Glass and M. J. Zwart, *Geol. Soc. Am. Bull.* **90**, 595 (1979); B. P. Glass, *Earth Planet. Sci. Lett.* **16**, 23 (1972).
13. E. C. T. Chao, in *Tektites*, J. A. O'Keefe, Ed. (Univ. of Chicago Press, Chicago, 1963), pp. 51–94.
14. The oxide variation patterns of the Qidong microspherules presented in Fig. 6 are distinct from those documented for the Cynthia glasses that were believed to be fly ash spherules [G. B. Byerly, J. E. Hazel, C. McCabe, *Meteoritics* **25**, 89 (1990)].
15. Natural glasses are known to be thermodynamically unstable; with time and under a variety of conditions, they become crystalline. Water and temperature are important factors [R. R. Marshall, *Geol. Soc. Am. Bull.* **72**, 1493 (1961)].
16. Volcanic glass shards may contain as much as 5% water [G. A. Izatt, *J. Geophys. Res.* **96**, 20894 (1991), and references therein].
17. Although rare, there are reports of unaltered volcanic glasses of Precambrian [H. C. Palmer, K. Tazaki, W. S. Fyte, Z. Zhon, *Geology* **16**, 221 (1988)], Carboniferous [H. U. Schimincke and G. Pritchard, *Naturwissenschaften* **68**, 615 (1981)], Triassic [D. A. Brew and L. J. P. Muffler, *U.S. Geol. Surv. Prof. Pap.* **525C** (1966), p. 38], and Jurassic [J. W. Shervais and B. B. Hanan, *Geology* **17**, 510 (1989)] age.
18. Petrographic examination of thin sections of the limestone indicates that it underwent several stages of diagenesis.
19. The compositions of impact glasses may reflect those of target rocks. A target of a sedimentary rock assemblage of arkose, dolomite (high CaO content and high MgO/FeO ratios), and shale (high Al_2O_3 content) could account for the compositions of the microspherules. The observed silica inclusions could be derived from the arkose as a result of the partial melting of quartz grains in a molten melt after the impact. The high-silica glass could result from chemical reaction or incomplete mixing between the original impact melt and included silica.
20. B. P. Glass, C. A. Burns, J. R. Crosbie, D. L. DuBois, *J. Geophys. Res.* **90**, D175 (1985).
21. W. A. Cassidy, B. P. Glass, B. C. Heezen, *ibid.* **74**, 1009 (1969).
22. B. P. Glass and P. A. Zwart, *Earth Planet. Sci. Lett.* **43**, 336 (1979).
23. I thank D. J. McLaren and S. Bai for help and advice during the 1987 field trip to Qidong, China; B. P. Glass for providing important information on microtektites and volcanic glasses; J. M. Arocena for the XRMD analysis; B. D. E. Chatterton, A. Locock, and H. H. J. Geldsetzer for their support and help; and R. StJ. Lambert, R. W. Luth, and A. Locock for helpful comments on early drafts.

24 February 1992; accepted 20 April 1992

In Vivo Gene Transfer with Retroviral Vector–Producer Cells for Treatment of Experimental Brain Tumors

Kenneth W. Culver,* Zvi Ram, Stuart Wallbridge, Hiroyuki Ishii, Edward H. Oldfield, R. Michael Blaese

Direct in situ introduction of exogenous genes into proliferating tumors could provide an effective therapeutic approach for treatment of localized tumors. Rats with a cerebral glioma were given an intratumoral stereotaxic injection of murine fibroblasts that were producing a retroviral vector in which the herpes simplex thymidine kinase (HS-tk) gene had been inserted. After 5 days during which the HS-tk retroviral vectors that were produced in situ transduced the neighboring proliferating glioma cells, the rats were treated with the anti-herpes drug ganciclovir. Gliomas in the ganciclovir- and vector-treated rats regressed completely both macroscopically and microscopically. This technique exploits what was previously considered to be a disadvantage of retroviral vectors—that is, their inability to transfer genes into nondividing cells. Instead, this feature of retroviruses is used to target gene delivery to dividing tumor cells and to spare nondividing neural tissue.

Direct transfer of specific tumor suppressor genes, of genes that encode a particular toxic product, or of genes whose products specifically induce apoptosis in the tumor cells could be important approaches for treating malignancy. Retroviral-mediated gene transfer, the current method of choice for clinical gene transfer, has been limited in its usefulness because murine retroviruses stably integrate their genes only in target cells that are actively synthesizing DNA (*1*). Thus, attempts at retrovirus-mediated gene transfer into cell types that are usually in G_0, such as the totipotent bone marrow stem cell, have had only limited success. We considered the possibility that the requirement for target cell DNA synthesis could be exploited to limit gene delivery to proliferating tumor cells present in an organ in which the resident normal cells are not proliferating. The optimal method of gene transfer to a growing tumor would provide for the continuous delivery of retroviral particles into the immediate local environment of the tumor so that when an individual tumor cell enters DNA synthesis, a vector particle is available to transduce it. Continuous local infusion of retroviral vector–containing supernatants might be possible, although technically difficult. Our approach was to infiltrate the tumor mass with cells engineered to actively produce retroviral vector particles so that continuous production of the vector occurred within the tumor mass in situ.

K. W. Culver, H. Ishii, R. M. Blaese, Cellular Immunology Section, Metabolism Branch, National Cancer Institute, National Institutes of Health, Bethesda, MD 20892.
Z. Ram, S. Wallbridge, E. H. Oldfield, Surgical Neurology Branch, National Institute of Neurologic Disorders and Stroke, National Institutes of Health, Bethesda, MD 20892.

*To whom correspondence should be addressed.

We designed our initial experiments to determine if retroviral-mediated gene transfer after reimplantation of mixtures of tumor cells with vector-producing fibroblasts could be successfully accomplished in vivo. Mice were inoculated subcutaneously with fibrosarcoma cells mixed with either control fibroblasts that expressed the neomycin resistance gene (NeoR) (3T3 cells not producing retroviral vectors) or 3T3 cells that produce the NeoR retroviral vector (PA317) (*2*). To measure the efficiency of gene transfer in vivo, we resected the tumors after 4 weeks, reestablished them in culture, and then tested them in a clonogenic assay for expression of the NeoR gene by culture with the neomycin analog G418 (Table 1). No G418-resistant tumor colonies were recovered from any animal that received control fibroblasts. By contrast, 63 ± 9% (mean ± SEM) of the tumor cells recovered from animals injected with the tumor mixed with retroviral vector–producing fibroblasts grew as G418-resistant colonies in a clonogenic assay, which indicated that in vivo gene transfer into the proliferating tumor cells had been accomplished. Southern (DNA) blot analysis for the NeoR vector and a direct enzyme assay for neomycin phosphotransferase were positive in all these G418-resistant tumor cell populations (*3*). These experiments clearly indicate that proliferating tumor cells can be successfully transduced in vivo if mixed with retroviral vector–producing cells.

Several gene transfer systems might be useful for the local treatment of cancer. Increasing the immunogenicity of tumors by causing local cytokine production or by enhancement of major histocompatibility complex antigen expression can lead to local antitumor effect (*4*). Another approach is the introduction of a gene that